

# Theoretical studies and antibacterial activity for Schiff base complexes

Wail Al Zoubi<sup>1</sup>  | Abbas Ali Salih Al-Hamdani<sup>2</sup> | I Putu Widiyantara<sup>1</sup> | Rehab Ghalib Hamoodah<sup>2</sup> | Young Gun Ko<sup>1</sup>

<sup>1</sup>School of Materials Science and Engineering, Yeungnam University, Gyeongsan 38541, Republic of Korea

<sup>2</sup>Department of Chemistry, College of Science for Women, University of Baghdad, Baghdad, Iraq

## Correspondence

Young Gun Ko, School of Materials Science and Engineering, Yeungnam University, Gyeongsan 38541, Republic of Korea.  
Email: younggun@ynu.ac.kr

## Abstract

New ligand 4-((2-Hydroxy-1-naphthyl) methylene amino)-1.5-dimethyl-2-phenyl-1H-pyrazol-3(2H)-one (HL) was synthesized from the reaction of 2-hydroxy-1-naphthaldehyde and 4-aminophenaz one. A complexes of this ligand [VO(II)(HL)(SO<sub>4</sub>)], [Pt(IV)(L)Cl<sub>3</sub>], [Re(V)(L)Cl<sub>3</sub>]Cl, and [M(II)(L)Cl] (M=Pd(II), Ni(II), Cu(II)) were synthesized. The resulted compounds were characterized by IR, NMR (<sup>1</sup>H and <sup>13</sup>C), mass spectrometry, element analysis, and UV-Vis spectroscopy. Additionally, the spectroscopic studies revealed octahedral geometries for the Re(V), Pt(IV) complexes, and square pyramidal for VO(II), square planar for Pd(II) complex, and tetrahedral for the Ni(II) and Cu(II) complexes. Thermodynamic parameters ( $\Delta E^*$ ,  $\Delta H^*$ ,  $\Delta S^*$ ,  $\Delta G^*$ , and K) were calculated using from the TGA curve Coats-Red fern method. Therefore, hyper Chem-8 program has been used to predict structural geometries of compounds in the gas phase. Finally, the synthesized Schiff base and its metal complexes were screened for their biological activity against bacterial species, 2 Gram-positive bacteria (*Bacillus subtilis* and *Staphylococcus aureus*) and 2 Gram-negative bacteria (*Escherichia coli* and *Pseudomonas aeruginosa*).

## KEYWORDS

2-hydroxy-1-naphthaldehyde, theoretical studies, thermal analysis, transition metal complexes

## 1 | INTRODUCTION

The Schiff bases (also known as imine or azomethine) are common ligands in coordination chemistry. Schiff bases ligands are easily prepared and form complexes with almost all metal ions. Schiff bases are known to be a sort of ligands with strong coordinative ability, and almost all SBs can form 1:1 complexes with transition metal ions.<sup>[1]</sup> Besides interesting structural features, Schiff bases complexes revealed catalytical activity and some complexes are used as components in the preparation of thin-film organic solar cells or self-assembling layers.<sup>[2]</sup> Schiff bases have aroused many investigators' interests because of their readiness to chelate as bidentate ligands, through the nitrogen and oxygen atoms,

with various transition metal ions. Tridentate Schiff bases with nitrogen, oxygen, and sulfur donor atoms have shown good coordination with various metal ions, rendering tremendous attraction.<sup>[3,4]</sup>

The coordination of Schiff bases (2-[(N,N-dimethylaminophenylimino)-methyl]-4-xphenol) toward metal ions can enhance or minimize their activities.<sup>[5]</sup> Schiff bases are a class of ligands capable of forming coordinate bonds with many of metal ions through both azomethine group and phenolic group or via its azomethine or phenolic groups.<sup>[6-9]</sup> Heterocyclic Schiff bases and their complexes receive significant interest and attention of inorganic biochemists and organic chemistry because of their biological activity including

antitumor, antibacterial, fungicidal, and anticarcinogenic properties.<sup>[10–13]</sup>

In this paper, we report the synthesis, thermal analysis, theoretical studies, and antibacterial screening of new transition metal complexes of Pd(II), Ni(II), Pb(II), and Cu(II) with Schiff bases derived from condensation of 2-hydroxy-1-naphthaldehyde and 4-aminophenaz. The complexes have been characterized by several tools of analyses such as elemental analyses, IR, and UV-Vis spectra as well as thermal gravimetric (TG) analysis. These complexes were assayed by the disk diffusion method for antibacterial and antifungal activity and compared with that of free Schiff bases.

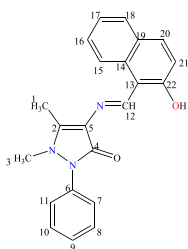
## 2 | EXPERIMENTAL

### 2.1 | Materials and methods

All chemicals were purchased from commercial sources and were used without further purifications (CaCl<sub>2</sub>, VOSO<sub>4</sub>.H<sub>2</sub>O, NiCl<sub>2</sub>.6H<sub>2</sub>O, PdCl<sub>2</sub>, CuCl<sub>2</sub>, ReCl<sub>5</sub>, H<sub>2</sub>PtCl<sub>6</sub>.6H<sub>2</sub>O, 2-hydroxy-1-naphthaldehyde, 4-aminophenazone, DMSO, CH<sub>3</sub>OH, and C<sub>2</sub>H<sub>5</sub>OH from Merck).

### 2.2 | Physical measurements

The electronic spectra were obtained by positive electron impact and fast atom bombardment was recorded on a VG



**SCHEME 1** Structure of 4-((2-Hydroxy-1-naphthyl) methylene amino)-1,5-dimethyl-2-phenyl-1H-pyrazol-3(2H)-one (HL)

auto spec micromass spectrometer. The IR spectra (KBr disc) were recorded on a JASCO FT-IR 410 spectrophotometer in the range of 4000 to 400 cm<sup>-1</sup>. <sup>1</sup>H NMR spectra were recorded in DMSO with TMS as an internal standard on a Joel GSX-400 MHz, FT NMR spectrophotometer. The UV-Vis measurements were recorded on a Perkin-Elmer k 20 UV-Vis Spectrometer. Conductivity measurements were made with DMSO solutions using a Jenway 4071 digital conductivity meter at room temperature. Chlorine was determined using potentiometer titration method on a 686-Titro processor-665Dosimat-Metrohm Swiss. Microanalyses were obtained with an Elemental analyses system a Perkin-Elmer automatic equipment model 240 B. Melting points were recorded on an Electrothermal 9200 apparatus and are uncorrected. Metal ions were determined using a Shimadzu (A.A) 680 G atomic absorption Spectrophotometer. Magnetic moments were measured with a magnetic susceptibility balance (Jonson Matthey Catalytic System Division), and thermal analysis studies of the compounds were performed on a Perkin-Elmer Pyris Diamond DTA/TG thermal system under nitrogen atmosphere at a heating rate of 10°C/min from 25 to 700°C.

### 2.3 | Synthesis of Schiff base (HL)

The ligand (Scheme 1) was prepared by condensing 2-hydroxy-1-naphthaldehyde in hot ethanolic solution of 4-aminophenazone in 1:1 molar ratio, and then, the reaction mixture was heated to reflux for 3 hours. The <sup>1</sup>H NMR spectra of the Schiff base provide compelling evidence of the presence of azomethine group. The product was dried and crystallized from a mixture (water: ethanol) (1:1) at room temperature.

Yield: 90%, mp = 212°C. <sup>1</sup>H NMR (Figure 1) (DMSO, ppm): 9.08 (s, -CH=N, <sup>1</sup>H), 7.08 to 7.98 (m, arom), 10.99 (s, -OH, 1H), 3.1 (s, CH<sub>3</sub>, 3H), 3.39 (s, CH<sub>3</sub>, 3H), (2.5, DMSO). <sup>13</sup>C NMR (Figure 2) (DMSO, ppm): 161.3 (-CH=N), 111 to 136 (arom), 27.04 (C-CH<sub>3</sub>), 59.33(N-CH<sub>3</sub>). FTIR (Figure 2) (cm<sup>-1</sup>): 3051 and 3024 (CH aromatic), 1639 (CH=N stretching), 1747 (C=O). The series

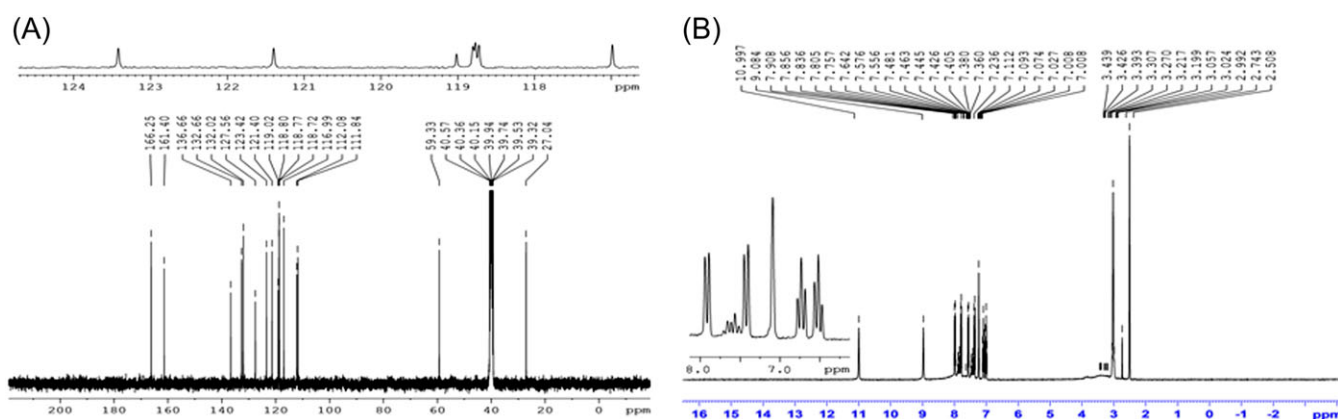


**FIGURE 1** A, <sup>1</sup>H NMR and B, <sup>13</sup>C NMR spectra of Schiff base

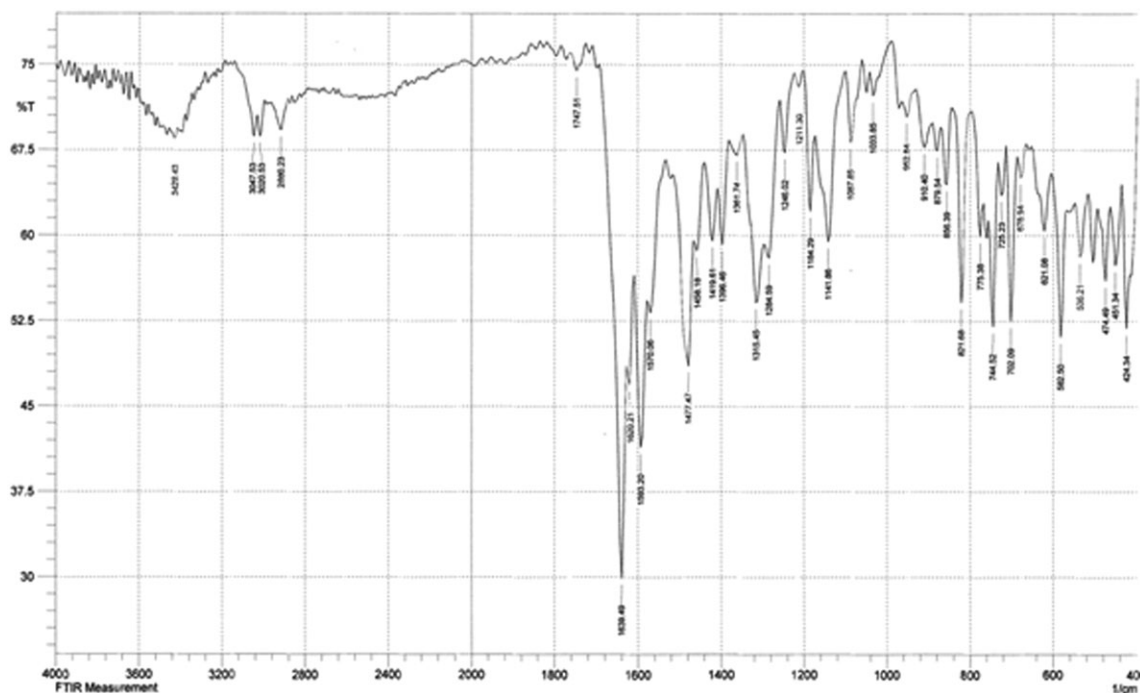


FIGURE 2 The FT-IR spectra of Schiff base

of peaks (Figure 3) in the range, ie, 67, 96, 138, 158, 212, and 357 amu, may be assigned to fragments.

## 2.4 | Synthesis of Schiff base complexes

Ni(II), Cu(II), Pd(II), Vo(II), Re(V), and Pt(IV) complexes (Scheme 2) were prepared in a similar manner using the

method by Al Zoubi and Al-Hamdani. Thus, a solution of 4 mmol of metal salts in 10 mL of ethanol was added to an ethanol solution containing 1 mmol Ligand(L) and was refluxed for 5 hours. The resulting solution was concentrated to a small volume (3 mL) on a rotary evaporator, and the product was separated by the addition of small amount of pet-ether (Petroleum ether) (60-80°C) mixture. Elemental

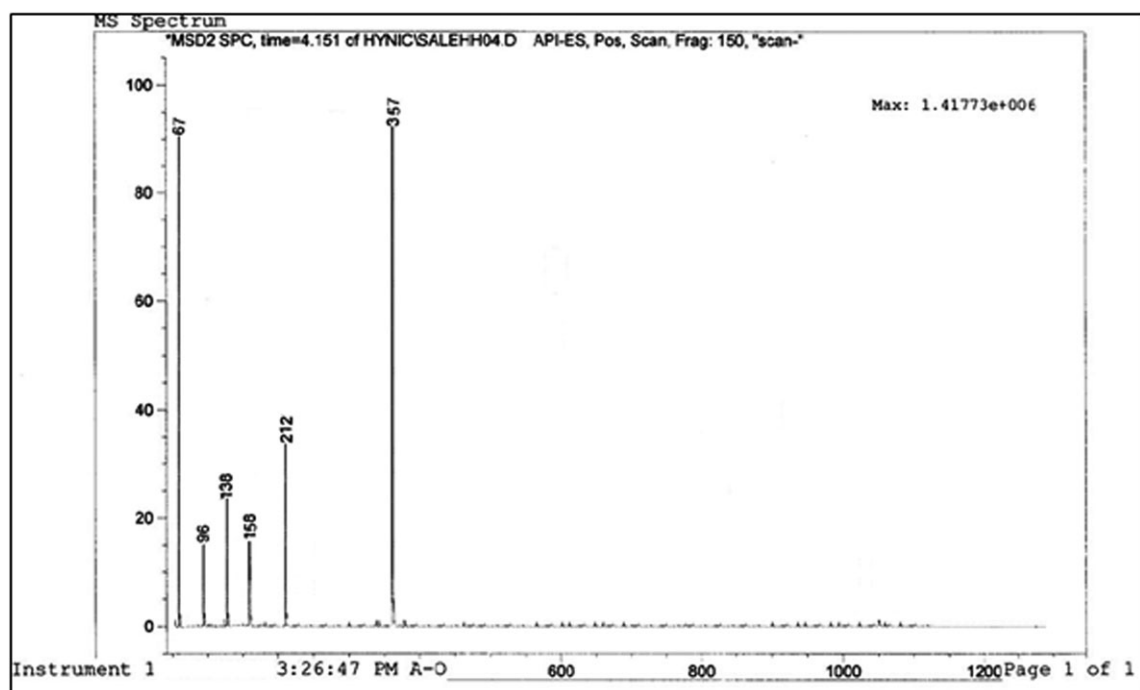
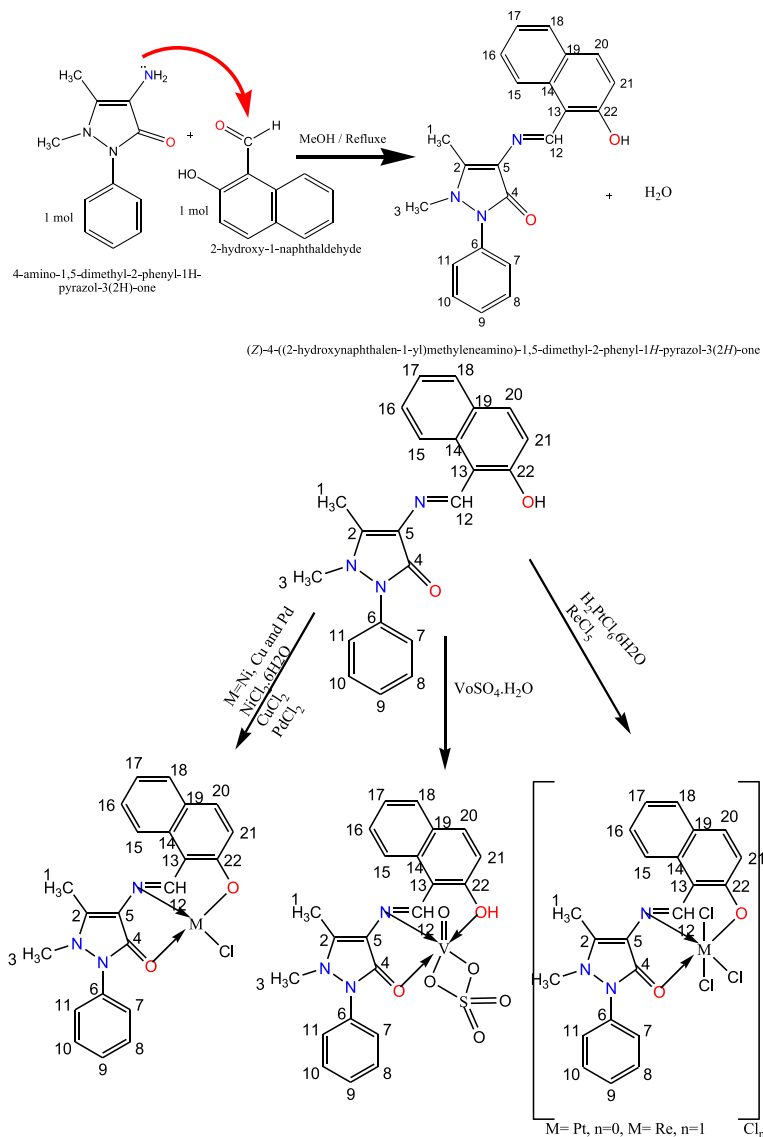


FIGURE 3 The MS spectra of Schiff base



**SCHEME 2** Preparation of Schiff base and its complexes

analysis, colors, and yields for the complexes are given in Table 1.

## 2.5 | Programs used in theoretical calculation

Hyper Chem-8 program is a sophisticated molecular modeler, editor, and powerful computational package that are known for its quality, flexibility, and ease of use, uniting 2D visualization and animation with quantum chemical calculations, molecular mechanics, and dynamics. In the present work, parameterization method 3 (PM3) was used for the calculation of the heat of formation and binding energy for all metal complexes. The (PM3) and (AMBER) are more popular than other semiempirical methods because of the availability of algorithms, and these are more accurate than other methods.<sup>[14]</sup> It has parameterized primarily for organic molecules and selected transition metals.<sup>[15]</sup>

## 2.6 | The thermal analysis

From the curves recorded for the successive steps in the decomposition process of these ligand and complexes, it was possible to determine the following characteristic thermal parameters for each reaction step: Initial point temperature of decomposition ( $T_i$ ): the point at which TG curve starts deviating from its base line. Final point temperature of decomposition ( $T_f$ ): the point at which TG curve returns to its base line. Peak temperature, ie, temperature of maximum rate of weight loss ( $T_{DTG}$ ): the point obtained from the intersection of tangents to the peak of TG curve. Mass loss at the decomposition step (Dm): It is the amount of mass that extends from the point  $T_i$  up to the reaction end point  $T_f$  on the curve, ie, the magnitude of the ordinate of a TG curve. The material released at each step of the decomposition is identified by attributing the mass loss (Dm) at a given step to the component of similar weight calculated from the molecular formula of the investigated complexes, comparing that with literatures of relevant

**TABLE 1** Colour, melting point, element microanalyses, and molar conductance values

Molecular Formula, $M_{wt}$	mp, °C	Colour	Element Microanalysis Found (Calcd), %					Molar Conductivity ( $\text{cm}^2 \cdot \Omega^{-1} \cdot \text{mol}^{-1}$ )
			M	C	H	H	Cl	
HL = $\text{C}_{22}\text{H}_{19}\text{N}_3\text{O}_2$ 357	212	Yellow crystals	-	73.92 (73.94)	4.88 (5.36)	4.88 (5.36)	-	-
VOHL = 520.41 $\text{C}_{22}\text{H}_{19}\text{N}_3\text{O}_7\text{VS}$	295-298d	Greenish yellow	10.0 (9.79)	51.09 (50.77)	3.11 (3.68)	3.11 (3.68)	-	7
NiL = 450.54 $\text{C}_{22}\text{H}_{18}\text{N}_3\text{O}_2\text{NiCl}_2$	265-267	Green	13.98 (13.03)	59.06 (58.65)	4.87 (4.03)	4.87 (4.03)	8.08 (7.87)	12
CuL = 455.40 $\text{C}_{22}\text{H}_{18}\text{N}_3\text{O}_2\text{CuCl}_2$	250-252	Greenish yellow	14.14 (13.95)	58.77 (58.02)	4.44 (4.98)	4.44 (4.98)	8.54 (7.79)	15
PdL = 498.27 $\text{C}_{22}\text{H}_{18}\text{N}_3\text{O}_2\text{PdCl}_2$	239-241d	Yellow brown	22.11 (21.36)	53.88 (53.03)	4.22 (3.64)	4.22 (3.64)	7.77 (7.12)	9
Pt L = 657.83 $\text{C}_{22}\text{H}_{18}\text{N}_3\text{O}_2\text{PtCl}_3$	277-278d	Dark brown	30.33 (29.65)	41.0 (40.17)	3.08 (2.76)	3.08 (2.76)	16.12 (16.17)	13
Re L = 684.42 $\text{C}_{22}\text{H}_{18}\text{N}_3\text{O}_2\text{ReCl}_4$	256-257d	Greenish	-	39.03 (38.61)	3.33 (2.65)	3.33 (2.65)	21.08 (20.72)	30

Abbreviation: d, decomposition.

compounds considering their temperature. This may assist identifying the mechanism of reaction in the decomposition steps taking place in the complexes under study. Activation energy (E) of the composition step: The integral method used is the Coats-Red fern equation,<sup>[14]</sup> for reaction order  $n \neq 1$  or  $n = 1$ , which when linear Z for a correctly chosen n yields the activation energy from the slope. The equations are given below: by plotting the appropriate left-hand side of the below equations  $1/T$ , the slope equals  $-E/2.303R$ .

$$\text{Log} \left[ \frac{1-(1-\alpha)^{1-n}}{T^2(1-n)} \right] = \text{Log} \left[ \left( 1 - \frac{2RT}{E_a} \right) \right] - \frac{E_a}{2.303RT} \text{ for } n \neq 1,$$

$$\text{Log} \left[ \frac{-\log(1-\alpha)}{T^2} \right] = \text{Log} \left[ \frac{ZR}{qE_a} \left( 1 - \frac{2RE}{E_a} \right) \right] - \frac{E_a}{2.303RT} \text{ for } n = 1.$$

$\Delta S^* = 2.303R [\log (Ah/KT_{\max})]$ ,  $\Delta H^* = E - RT_{\max}$ ,  $\Delta G^* = \Delta H^* - T_{\max} \cdot \Delta S^*$ , where  $\alpha$  = fraction of weight loss, T = temperature (K), n = order of reaction, A or Z = pre-exponential factor, R = molar gas constant, E = activation energy, and q = heating rate. Order of reaction (n): It is the one for which a plot of the Coats-Red fern expression gives the best straight line among various trial values of n that are examined relative to that estimated by the Horovitz-Metzger method.<sup>[16]</sup>

**TABLE 2** The important infrared frequencies ( $\text{cm}^{-1}$ ) of Schiff base and its complexes

Compound Name	$\nu(\text{C}=\text{O})$	$\nu(\text{C}=\text{N})$	H-bonded $\nu(\text{OH})$ Stretching	$\nu(\text{M}-\text{N})$	$\nu(\text{M}-\text{O})$	Other Bands
HL	1747	1639	3429			$\nu(\text{C}-\text{H}) = 3047$ arom $\nu(\text{C}-\text{H}) = 2880$ aliph
[CuL <sub>2</sub> Cl]	1690	1616	-	455	428	$\nu(\text{C}-\text{H}) = 3051$ arom $\nu(\text{C}-\text{H}) = 2943$ aliph
[NiL <sub>2</sub> Cl]	1689	1615	-	456	425	$\nu(\text{C}-\text{H}) = 3055$ arom $\nu(\text{C}-\text{H}) = 2943$ aliph
[PdL <sub>2</sub> Cl]	1785	1615	-	450	427	$\nu(\text{C}-\text{H}) = 3049$ arom $\nu(\text{C}-\text{H}) = 2943$ aliph
[PtL <sub>2</sub> Cl <sub>3</sub> ]	1694	1613	-	469	418	$\nu(\text{C}-\text{H}) = 3059$ arom $\nu(\text{C}-\text{H}) = 2943$ aliph
[ReL <sub>2</sub> Cl <sub>3</sub> ]Cl	1700	1616	-	647	417	$\nu(\text{C}-\text{H}) = 3059$ arom $\nu(\text{C}-\text{H}) = 2943$ aliph
[VOHL <sub>2</sub> (SO <sub>4</sub> )]	1734	1670 1629	3399	478	428	$\nu(\text{C}-\text{H}) = 3020$ arom $\nu(\text{C}-\text{H}) = 2934$ aliph, $\nu(\text{V}=\text{O}) = 972$ $\nu(\text{SO}_4) = 914, 1033, 1088, \text{ and } 1184$

### 3 | RESULTS AND DISCUSSION

All the complexes are amorphous powder, insoluble in water and ether whereas soluble in solvents such as  $\text{CHCl}_3$ ,  $\text{CH}_2\text{Cl}_2$ , MeCN, DMF, and DMSO. The molar conductance data (Table 1) indicate that all the complexes are nonelectrolytes (Scheme 2).<sup>[17]</sup>

The ligand was characterized by elemental analysis (Table 1). IR (Table 2). and UV-Vis (Table 3). respectively. Monomeric complexes of the ligand with V(IV), Ni(II), Cu(II), Pd(II), Re(V), and Pt(IV) were synthesized by heating 1 mmol of the ligand with 1 mmol of metal salt using ethanolic solution. However, deprotonation of the ligand occur facilitating the formation of the complexes  $[\text{VO}(\text{II})(\text{HL})(\text{SO}_4)]$ ,  $[\text{Pt}(\text{IV})(\text{L})\text{Cl}_3]$ ,  $[\text{Re}(\text{V})(\text{L})\text{Cl}_3]$

Cl, and  $[\text{M}(\text{II})(\text{L})\text{Cl}]$  ( $\text{M}=\text{Ni}(\text{II})$ ,  $\text{Cu}(\text{II})$  and  $\text{Pd}(\text{II})$ ) (Scheme 2).<sup>[18]</sup>

The complexes are air-stable solids, solution in DMF and DMSO, sparingly soluble in MeOH,  $\text{CHCl}_3$ , and  $\text{CH}_2\text{Cl}_2$ . The analytical data (Table 1) agree well with the suggested

**TABLE 4** The fragmentation pattern data for the Schiff base

Ligand	Assignment	Peak, m/z	Relative Abundance, %
HL	$\text{M}=(\text{C}_{22}\text{H}_{19}\text{N}_3\text{O}_2)$	357	94
	$\text{M}-\text{C}_{12}\text{H}_7\text{O}^+=\text{M}_1$	212	34
	$\text{M}_1-\text{C}_4\text{H}_5^+=\text{M}_2$	158	17
	$\text{M}_2-\text{NH}_5^+=\text{M}_3$	138	24
	$\text{M}_3-\text{CNO}=\text{M}_4$	96	15
	$\text{M}_4-\text{CH}_2\text{N}^+$	67	91

**TABLE 3** Magnetic and spectra data of the ligand and its metal complexes

Complex geometry	$\Lambda_m \cdot \text{cm}^2 \cdot \Omega^{-1} \cdot \text{mol}^{-1}$	$\mu_{\text{eff}}$ B.M	$\nu$ ( $\text{cm}^{-1}$ )	ABS	$\lambda_{\text{max}}$ , nm	$\epsilon_{\text{max}} \cdot \text{L} \cdot \text{mol}^{-1} \cdot \text{cm}^{-1}$	Assignments
[VOHL <sub>2</sub> (SO <sub>4</sub> )] (Sqy)	7	1.77	37 174.7	1.685	269	16 850	Ligand field
			30 769.2	1.381	325	13 810	Ligand field
			29 673.5	1.392	337	13 920	Ligand field
			25 641	2.101	390	21 010	C.T
			19 305	0.111	518	111	<sup>2</sup> B <sub>2</sub> → <sup>2</sup> B <sub>1</sub>
			12 610	0.078	793	78	<sup>2</sup> B <sub>2</sub> → <sup>2</sup> E
[NiL <sub>2</sub> Cl](Th)	12	2.80	37 174.7	1.393	269	13 930	Ligand field
			30 395	1.040	329	1040	Ligand field
			29 585.7	1.082	338	1082	Ligand field
			25 575.4	2.039	391	2039	Ligand field
			18 181.8	0.055	550	550	M → L(C.T)
			13 869.6	0.061	721	61	<sup>3</sup> T <sub>1</sub> → <sup>3</sup> T <sub>2</sub>
			10 204	0.054	980	54	<sup>3</sup> T <sub>1g</sub> → <sup>3</sup> T <sub>1</sub> (P)
[CuL <sub>2</sub> Cl](Th)	15	1.68	36 496	1.407	274	1407	Ligand field
			28 985.5	0.856	345	856	Ligand field
			23 419	1.203	427	12 030	C.T
			12 642	0.036	791	360	<sup>2</sup> T <sub>2</sub> → <sup>2</sup> E
[Pd L <sub>2</sub> Cl](Sq)	9	dia	37 174.7	1.603	269	16 030	Ligand field
			30 674.8	1.183	326	11 830	Ligand field
			29 585.7	1.167	338	11 670	Ligand field
			24 630.5	2.306	406	2306	M → L(Ct)
			16 949	0.201	590	201	<sup>1</sup> A <sub>1g</sub> → <sup>1</sup> B <sub>1g</sub> ν <sub>2</sub>
			12 626	0.198	792	198	<sup>1</sup> A <sub>1g</sub> → <sup>1</sup> A <sub>2g</sub> ν <sub>1</sub>
[PtL <sub>2</sub> Cl <sub>3</sub> ](Oh)	13	dia	36 496	2.072	274	20 720	Ligand field
			28 985.5	2.217	345	22 170	Ligand field
			25 510	2.421	392	2421	Ligand field + (CT)
			17 094	0.621	585	621	<sup>1</sup> A <sub>1g</sub> → <sup>1</sup> T <sub>3g</sub>
			14 326.6	0.465	698	465	<sup>1</sup> A <sub>1g</sub> → <sup>1</sup> T <sub>2g</sub>
			12 150.6	0.248	823	248	<sup>1</sup> A <sub>1g</sub> → <sup>1</sup> T <sub>1g</sub>
[ReL <sub>2</sub> Cl <sub>3</sub> ]Cl(Oh)	30	3.05	36 496	2.072	274	20 720	Ligand field
			28 985.5	2.217	345	22 170	C.T
			25 510	2.421	392	242	<sup>3</sup> T <sub>1g</sub> → <sup>3</sup> A <sub>2g</sub>
			19 762.8	0.301	506	301	<sup>3</sup> T <sub>1g</sub> → <sup>3</sup> T <sub>1g</sub> (P)
			13 947	0.018	717	180	<sup>3</sup> T <sub>1g</sub> → <sup>3</sup> T <sub>2g</sub> (F)

Abbreviations: dia, diamagnetic; Oh, octahedral; Sp, square planar; Spy, square pyramidal; Th, tetrahedral.

formulae. The most important infrared bands of the ligand and its complexes together with their assignments are collected in Table 2.

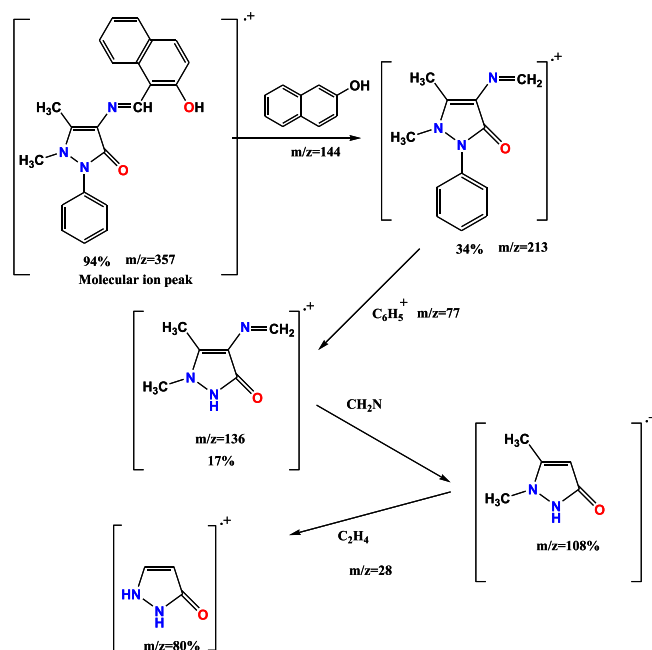
### 3.1 | The IR spectra

All peculiar features of the Infrared spectra are consistent with the structural characteristics of the Schiff base and its metal complexes. A characteristic stretching vibration (Table 2) was observed in the region 1619 to 1640  $\text{cm}^{-1}$  attributed to  $\nu(\text{C}=\text{N})$ . The broad bands around 3200 to 3429  $\text{cm}^{-1}$  are assigned to H-bonded  $-\text{OH}$  stretching vibrations; a strong band at 1720 to 1747  $\text{cm}^{-1}$  and 1281 to 1284  $\text{cm}^{-1}$  in the IR spectra of the Schiff bases are assigned to  $\nu(\text{C}=\text{O})$  and phenolic  $\nu(\text{C}-\text{O})$  vibrations, respectively. In comparison with the vibrational spectra (Table 2) of the metal complexes with the free ligands, the  $\nu(\text{C}=\text{N})$  and  $\nu(\text{C}=\text{O})$  are shifted to the lower wave number ( $(\text{C}=\text{N})$  (28–22  $\text{cm}^{-1}$ ) ( $\text{C}=\text{O}$ ) (57–13  $\text{cm}^{-1}$ )), ie, in the range 1590 to 1593  $\text{cm}^{-1}$  shows the coordination of nitrogen of azomethine group to the metal ion. This indicates that the ligand was coordinated with the metal ions through the imine and carbonyl group. The metal complexes (as shown in Table 2) showing broad

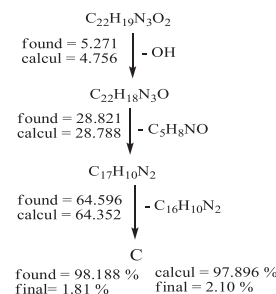
band in the region 3375 to 3399  $\text{cm}^{-1}$  and 2 weak bands in the region 700 to 720  $\text{cm}^{-1}$  and 752 to 801  $\text{cm}^{-1}$  are attributed to the presence of coordinated water molecules because of  $\nu(\text{OH})$  rocking and wagging modes of vibrations, respectively.<sup>[19–21]</sup> The reduction in bond order, upon complexation, can be attributed to delocalization of metal electron density ( $t_{2g}$ ) to the  $\pi$ -system of the ligand. These shifts confirm the coordination of the ligand via the nitrogen of the azomethine group and oxygen of carbonyl and the phenol groups to metal ions. At lower frequency the complexes exhibited bands around 478 to 447  $\text{cm}^{-1}$  assigned to the  $\nu(\text{M}-\text{N})$  and exhibited bands around 428 to 417  $\text{cm}^{-1}$  assigned to the  $\nu(\text{M}-\text{O})$  for complexes and new bands in  $[\text{VOHL}(\text{SO}_4)]$  complex the 927  $\text{cm}^{-1}$  assigned to the  $\nu(\text{V}=\text{O})$ . This indicates that the ligand was coordinated with the V(IV) ion through the O atom and 1103, 1084, and 1022  $\text{cm}^{-1}$  assigned to the  $\nu(\text{SO}_4)$ . This indicates that the  $\text{SO}_4$  was coordinated with the V(IV) ion through the mono O atom (mono dentate).<sup>[17,22]</sup> All these data are shown in Table 2.

### 3.2 | Electronic spectra studies

The electronic spectral values of ligand and its complexes are recorded in Table 3. The electronic spectra of VO complexes generally showed 3 absorption bands in the region at 790, 518, and 390 nm, which are assigned to transitions  ${}^2\text{B}_2 \rightarrow {}^2\text{E}$ ,  ${}^2\text{B}_2 \rightarrow {}^2\text{B}_1$ , and  $\text{M} \rightarrow \text{L}(\text{C.T})$  showing a square pyramidal geometry<sup>[17,23]</sup> around the VO ion. The electronic spectral data of Ni(II) complexes showed d–d bands in the region 980, 721, and 550 nm, respectively, assigned to the transitions  ${}^3\text{T}_{1g} \rightarrow {}^3\text{T}_1(\text{P})$ ,  ${}^3\text{T}_1 \rightarrow {}^3\text{T}_2$ ,  $\text{M} \rightarrow \text{L}(\text{C.T})$ , which are characteristics of Ni(II) in tetrahedral geometry. The



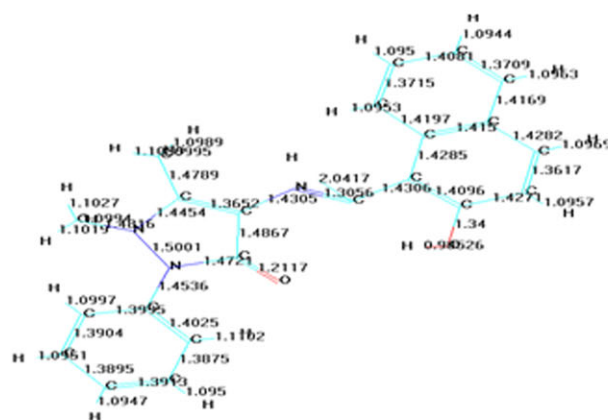
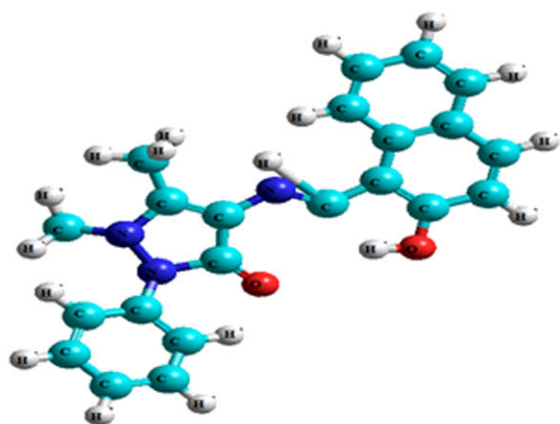
SCHEME 3 The proposed mass fragmentation pathways of ligand



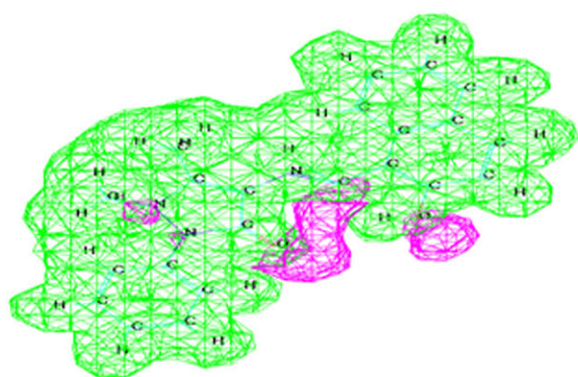
SCHEME 4 Proposed thermal decomposition pathways of Schiff base (HL)

TABLE 5 Thermal analysis results of thermal decomposition of the EB

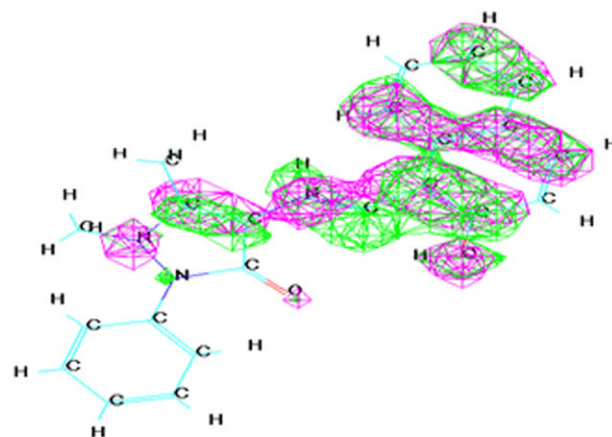
Ligand	Step	TGA			DTG		
		TG Range, °C	DTG <sub>max</sub> , °C	Mass Loss Calcd (Estim), %	Total Mass Loss	$\Delta\text{H}$ (kJ·mol <sup>-1</sup> )	T <sub>data</sub>
HL	1	33–121.7	68.7	4.756 (5.27)	98.188	endo	49.3
	2	122.1–429	368	28.788 (28.82)	97.896	endo	313
	3	460.3–689	654	64.352 (64.09)	97.896	endo	607



Ligand L



Electrostatic potential



HOMO &amp; LUMO = -8.217062 eV

FIGURE 4 Electrostatic potential (HOMO and LUMO) contours for ligand

electronic spectra of Cu(II) complexes exhibited low-energy absorption bands at 791 and 427 nm assigned to the transitions  ${}^2T_2 \rightarrow {}^2E$  and  $M \rightarrow L(C.T)$ . The high-energy band in the region at 345 to 269 nm is due to the forbidden ligand, on the basis of which a distorted octahedral geometry is suggested for Cu(II) complexes.<sup>[17]</sup> The electronic spectral data of Pd(II) complexes showed d-d bands in the region 792,

590, and 406 nm, respectively, assigned to the transitions  ${}^1A_{1g} \rightarrow {}^1A_{2g}$ ,  ${}^1A_{1g} \rightarrow {}^1B_{1g}$ ,  $M \rightarrow L(C.T)$ , which are characteristic of Pd(II) in square planar geometry.<sup>[24–27]</sup> In addition, The electronic spectral data of Pt(II) complexes showed d-d bands in the region 823, 698, 585, and 392 nm, respectively, assigned to the transitions  ${}^1A_{1g} \rightarrow {}^1T_{1g}$ ,  ${}^1A_{1g} \rightarrow {}^1T_{2g}$ ,  ${}^1A_{1g} \rightarrow {}^1T_{3g}$ , and  $M \rightarrow L(C.T)$ , which are characteristic of

TABLE 6 Conformation energy analysis in (K J.Mol<sup>-1</sup>) for the ligand and its complexes

Complexes	Total Energy	Binding Energy	Heat of Formation	Electronic Energy	Dipole (Debyes)
HL	-91 542.629	-5133.684	73.9510	-740 230.728	6.297
[VOHL <sub>2</sub> (SO <sub>4</sub> )]		1042.548 (AMBER)			3.57
[NiL <sub>2</sub> Cl]	-119 271.432	-6453.444	-24.5877	-5697.32	2.96
[CuL <sub>2</sub> Cl]	-102 917.146	-5375.758	-21.0218	-867 067.15	2.88
[Pd L <sub>2</sub> Cl]	-103 087.391	-5397.259	-12.509	-879 579.67	3.42
[Pt L <sub>2</sub> Cl <sub>3</sub> ]		230.987 (AMBER)			40.15
[Re L <sub>2</sub> Cl <sub>3</sub> ]Cl		1542.548 (AMBER)			38.83

Pt(II) in octahedral geometry. Additionally, The electronic spectral data of Re(III) complexes showed d–d bands in the region 717, 506, 392, and 345 nm, respectively, assigned to the transitions  ${}^3T_{1g} \rightarrow {}^3T_{2g}$  (F),  ${}^3T_{1g} \rightarrow {}^3T_{1g}$  (P),  ${}^3T_{1g} \rightarrow {}^3A_{2g}$ , and  $M \rightarrow L(C.T)$ , which are characteristic of Re(II) in Octahedral geometry.<sup>[28–30]</sup>

### 3.3 | Mass spectra

The mass spectrum of the ligand HL is shown in Table 4 and Scheme 3, the peak at  $m/z = 357$  due to the molecular ion peak which coincides with its formula weight. The proposed fragmentation pattern of the ligand is given below (Scheme 3). The ligand spectrum shows  $M^+ - C_{12}H_7O$  and  $M^+ + C_4H_5$  peaks, which are characteristics of aromatic rings. Loss of one of the amino hydrogen atom of Schiff base gives a moderately intense  $M^+ - 1$  peak; this effect is more pronounced in amino group because of the better resonance stabilization of ion fragment by the nitrogen. This molecular ion peak also has the good agreement with nitrogen rule of molecular fragmentation as well as their calculated value of molar mass = 357.<sup>[31–34]</sup> The measured molecular weights were consistent with expected values and the mass spectrum of the complex is shown in Table 5 and Scheme 3.

### 3.4 | Thermal analysis studies

The thermal data of Scheme 4 and Table 5 refers to the decomposition of this Schiff base in 3 steps of total estimated mass loss of 100% (calcd 98.95%). The first step occurs within the temperature range 33.2°C to 121.7°C and exactly at 105.46°C (DTG) of estimated mass loss of 5.271%, (calcd 4.756%); which may be attributed to the decomposition of chemical formula OH (mole mass = 17). The second step occurs within the temperature range 122.1°C to 429°C and exactly at 323.28°C (DTG). It refers to the estimated mass loss of 28.821% (calcd 28.7), which may be attributed to the decomposition of chemical formula  $C_5H_8NO$  (mole mass = 98). Finally, the third step occurs within the temperature range 460.3°C to 689°C and exactly at 579.43°C (DTG). It refers to the estimated mass loss of 64.59% (calcd

64.352%), which may be attributed to the decomposition of chemical formula  $C_{16}H_{10}N_2$  (mole mass = 230).

### 3.5 | Electrostatic potentials

Electron distribution governs the electrostatic potential of the molecules. The electrostatic potential (E.P) describes the interaction of energy of the molecular system with a positive point charge. The E.P is useful for finding sites of reaction in a molecule; positively charged species tend to attack a molecule where the electro static potential is strongly negative (electrophonic attack).<sup>[23,24]</sup> The E.P of the free ligand was calculated and plotted as 2D contour to investigate the reactive sites of the molecules, Figure 3. Therefore, one can interpret the stereochemistry and rates of many reactions involving “soft” electrophiles and nucleophiles in terms of the properties of frontier orbital HOMO and LUMO. The results of calculations show that the LUMO of transition metal ions prefer to react with the HOMO of 3-donor atoms of 2 oxygen of carbonyl and nitrogen of imine group for free ligand (as shown in Figure 4).<sup>[24]</sup>

All theoretically probable structures of free ligand and their complexes have been calculated by (PM3) and (ZINDO/1) methods in the gas phase to search for the most probable model building stable structure, Table 6.

The vibrational spectra of the free ligand has been calculated, Table 7. The theoretically calculated wave numbers for this ligand showed that some deviations from the experimental values; these deviations are generally acceptable in theoretical calculations. Calculation of parameters has been optimized bond lengths of the free ligand and its metal complexes which to give excellent agreement with the experimental data as shown in Figure 5.

### 3.6 | Antibacterial activities

The newly synthesized compounds were screened for antibacterial activity. For antibacterial studies microorganisms such as *S. aureus* NCIM 2079, *Bacillus subtilis* NCIM 2063, *Escherichia coli* NCIM 2918, *P. aeruginosa* NCIM 2036 were used (Table 8) and assayed by minimum inhibitory concentration (MIC) by serial dilution technique. To

**TABLE 7** Comparison of experimental and theoretical vibrational frequencies for ligand

Ligand	$\nu(OH)$	$\nu(CH)$ aromatic	$\nu(CH)$ aliphatic	$\nu(CH)$ aldehyde	$\nu(C=O)$ ring	$\nu(C=N)$	$\nu(C-O-H)$
HL	3429 <sup>a</sup>	3047 <sup>a</sup>	2880 <sup>a</sup>	2924 <sup>a</sup>	1747 <sup>a</sup>	1639 <sup>a</sup> 1620 <sup>a</sup>	1087 <sup>a</sup>
	3444 <sup>b</sup>	3065 <sup>b</sup>	2976 <sup>b</sup>	2999 <sup>b</sup>	1777 <sup>b</sup>	1665 <sup>b</sup>	1203 <sup>b</sup>
		-0.590 <sup>c</sup>	-3.333 <sup>c</sup>	-2.564 <sup>c</sup>	-1.717 <sup>c</sup>	-0.21 <sup>c</sup>	-10.67 <sup>c</sup>

<sup>a</sup>Experimental frequency.

<sup>b</sup>Theoretical frequency.

<sup>c</sup>Error % due to main difference in the experimental measurements and theoretical treatments of vibration spectrum.

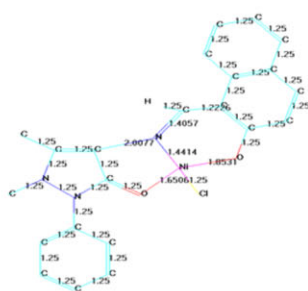
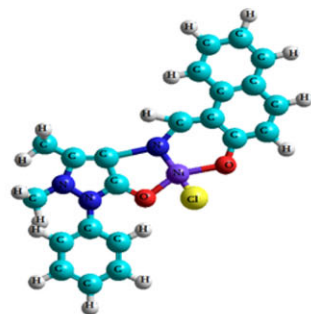
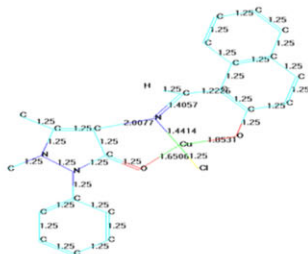
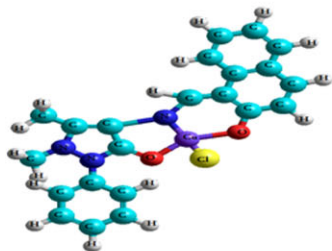
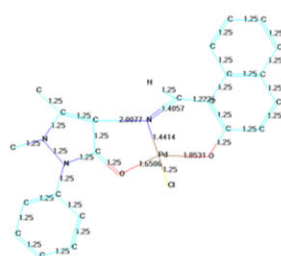
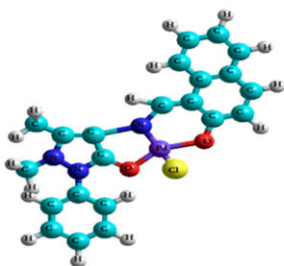
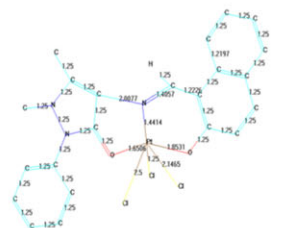
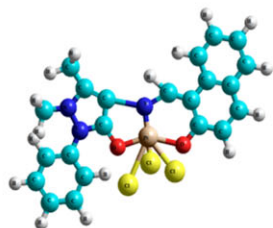
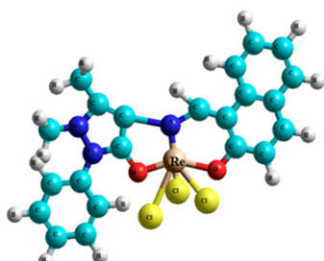
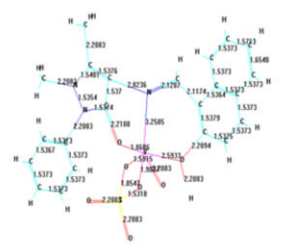
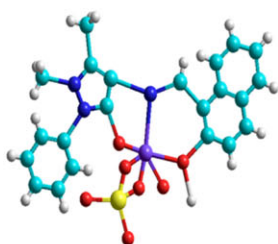
NiL<sub>2</sub>CuL<sub>2</sub>PdL<sub>2</sub>PtL<sub>2</sub>ReL<sub>2</sub>VOL<sub>2</sub>

FIGURE 5 Conformational structure of ligand and their metal complexes

**TABLE 8** Screening of minimal inhibitory concentration for sample with Gram-positive bacteria and Gram-negative bacteria

Compounds	Minimal Inhibitory Concentration, $\mu\text{g/mL}$									
	Gram-Positive Bacteria					Gram-Negative Bacteria				
	BS	SA	ES	PA	ES	PA	ES	PA	ES	PA
HL	1000	1000	1200	900						
[VOHL(SO <sub>4</sub> )	1800	1300	1800	1200						
[NiLCl]	2000	2000	1400	1400						
[CuLCl]	1600	1800	2000	1600						
[PdLCl]	2000	2000	2000	2000						
[PtLCl <sub>3</sub> ]	2000	2000	2000	1500						
[ReLCl <sub>3</sub> ]Cl	1200	2000	1600	1000						
Dilutions for MIC										
No of tubes for MIC	1	2	3	4	5	6	7	8	9	10
Concentration of drug ( $\mu\text{g/ml}$ )	4000	2000	1000	500	250	125	62.5	31.25	15.625	7.812

Abbreviations: BS, *Bacillus subtilis* NCIM 2063; EC, *Escherichia coli* NCIM 2911; PA, *Pseudomonas aeruginosa* NCIM 2036; SA, *Staphylococcus aureus* NCIM 2079.

determine the MIC, the compounds were dissolved in dimethyl sulfoxide. Ciprofloxacin was used as the standard and incubated for 24 hours at 37°C (Table 8).<sup>[17,20–24]</sup>

## 4 | CONCLUSION

In this paper, we have explored the synthesis and coordination chemistry of some monomeric complexes obtained from the reaction of the tridentate ligand L with some metal ions. The mode of bonding and overall structure of the complexes were determined through physicochemical and spectroscopic methods. Complexes formation study via molar ratio has been investigated, and results were consistent to those found in the solid complexes with a ratio of (M:L) as (1:1). The thermodynamic parameters, such as  $\Delta E^*$ ,  $\Delta H^*$ ,  $\Delta S^*$ ,  $\Delta G^*$ , and K are calculated from the TGA curve using Coats-Redfern method. Hyper Chem-8 program was used to predict structural geometries of compounds in the gas phase. The heat of formation ( $\Delta H_f$ ) and binding energy ( $\Delta E_b$ ) at 298 K for the A, free ligand, and its complexes were calculated by PM3 method. The synthesized ligand and its metal complexes were screened for their biological activity against bacterial species, 2 Gram-positive bacteria (*B. subtilis* and *S. aureus*) and 2 Gram-negative bacteria (*E. coli* and *P. aeruginosa*).

## REFERENCES

- W. Al Zoubi, N. Al Mhanna, *Spectrochim. Acta A* **2014**, *132*, 854.
- M. Barwiolek, M. Babinsk, A. Kozakiewicz, A. Wojtczak, A. Kaczmarek-Kedziera, E. Szlyk, *Polymer* **2017**, *124*, 12.
- W. Al Zoubi, Y. Gun Ko, *J. Organomet. Chem.* **2016**, *822*, 173.
- T. E. Olalekan, A. S. Ogunlaja, B. VanBrecht, G. M. Watkins, *J. Mol. Struct.* **2016**, *1122*, 72.
- R. A. Al-Hassani, M. M. Sinan, S. M. Abdullah, *Environ. Sci. Res.* **2013**, *1(6)*, 95.
- A. Muna, *Acta Chim. Pharm.* **2013**, *3(2)*, 127.
- A. A. S. Al-Hamdani, A. M. Balkhi, A. Falah, S. A. Shaker, *J. Saudi Chem. Soc.* **2016**, *20*, 487.
- C. Jayabalakrishnan, R. Karvembu, K. Natarajan, *Trans. Met. Chem.* **2002**, *27(1)*, 75.
- R. Prabhakaran, A. Geetha, M. Thilagavathi, R. Karvembu, V. Krishnan, H. Bertagnolli, K. Natarajan, *J. Inorg. Biochem.* **2004**, *98(12)*, 2131.
- K. P. Balasubramanian, R. Karvembu, R. Prabhakaran, V. Chinnusamy, K. Natarajan, *Spectrochim. Acta A* **2007**, *68(1)*, 50.
- S. A. Sadeek, M. S. Refat, *Korean Chem. Soc.* **2006**, *50(2)*, 107.
- R. J. Cozens, K. S. Murray, B. O. West, *J. Organomet. Chem.* **1971**, *27(3)*, 399.
- A. Bigotto, V. Galasso, G. Dealti, *Spectrochim. Acta A* **1972**, *28(8)*, 1581.
- A. A. S. Al-Hamdani, A. M. Balkhi, A. Falah, S. A. Shaker, *J. Chil. Chem. Soc.* **2015**, *60(1)*, 2774.
- R. Prabhakaran, R. Huang, K. Natarajan, *Inorg. Chim. Acta* **2006**, *359(10)*, 3359.
- A. A. S. Al-Hamdani, M. A. Mahmoud, S. H. R. Bakir, *Synthesis J. Baghdad for Sci* **2013**, *10(3)*, 583.
- A. W. Coats, J. P. Redfern, *Nature* **1964**, *201*, 68.
- W. Al Zoubi, A. Ali Salih Al-Hamdani, M. Kaseem, *Appl. Organomet. Chem.* **2016**, *30(10)*, 810.
- W. Al Zoubi, F. Karabet, R. Al Bandakji, K. Hussein, *Appl. Organomet. Chem.* **2017**, *31(2)*, 1.
- A. A. S. Al-Hamdani, W. Al Zoubi, *Spectrochim. Acta A* **2015**, *137*, 75.

- [21] H. A. Dorestt, A review of quantum chemical studies of energetic materials, **1996**. DSTO technical report.
- [22] J. C. Foresman, C. Frisch, Exploring Chemistry with Electronic Structure Methods second ed., Gaussian Inc., **1996**.
- [23] K. Singh, M. S. Barwa, B. P. Tyagi, *Eur. J. Med. Chem.* **2007**, *42*, 394.
- [24] K. Singh, M. Singh, B. P. Tyagi, *Eur. J. Med. Chem.* **2006**, *41*, 147.
- [25] G. Hoshina, M. Tsuchimoto, S. Ohba, K. Nakajima, H. Uekusa, Y. Ohasi, H. Ishida, M. Kojima, *Inorg. Chem.* **1998**, *37*, 142.
- [26] W. Al Zoubi, F. Kandil, M. K. Chebani, *Organic Chem Current Res.* **2012**, *1*(1), 1.
- [27] S. K. Sengupta, O. P. Pandey, J. K. Pandey, G. K. Pandey, *Indian J. Chem.* **2001**, *40A*.
- [28] A. Muna, *Acta Chim. Pharm. Indica.* **2013**, *3*(2), 127.
- [29] D. C. Young, *Computational Chemistry a practical Guide for Applying Techniques to realworld Problems*, John Wiley and Sons, Inc. publication, New York **2001**.
- [30] W. Al Zoubi, Y. G. Ko, *Appl. Organomet. Chem.* **2017**, *31*(3), 1.
- [31] A. A. S. Al-Hamdani, *Dirasat, Pure Scie* **2013**, *39*(1), 61.
- [32] A. A. S. Al-Hamdani, N. D. Shaalan, S. R. Bakir, M. S. Mohammed, *J. Baghdad Sci.* **2015**, *12*(2), 350.
- [33] W. Al Zoubi, F. Kandil, M. K. Chebani, *Arab. J. Chem.* **2016**, *9*(4), 526.
- [34] W. Al Zoubi, F. Kandil, M. K. Cheban, *Arab. J. Chem.* **2016**, *9*(5), 626.

**How to cite this article:** Al Zoubi W, Al-Hamdani AAS, Putu Widiyantara I, Hamoodah RG, Ko YG. Theoretical studies and antibacterial activity for Schiff base complexes. *J Phys Org Chem.* 2017;e3707. <https://doi.org/10.1002/poc.3707>